 CMES, vol.103, no.4, pp.229-249, 2014

Particle-based Simulations of Flows with Free Surfaces Using Hyperbolic-type Weighting Functions

K. Kakuda[1], **Y. Hayashi**[1] **and J. Toyotani**[1]

Abstract: In this paper, we present the application of the particle-based simulations to complicated fluid flow problem with free surfaces. The particle approach is based on the MPS (Moving Particle Simulation) method using hyperbolic-type weighting function to stabilize the spurious oscillatory solutions for solving the Poisson equation with respect to the pressure fields. The hyperbolic-type weighting function is constructed by differentiating the characteristic function based on neural network framework. The weighting function proposed herein is collaterally applied to the kernel function in the SPH-framework. Numerical results demonstrate the workability and validity of the present MPS approach through the dam-breaking flow problem.

Keywords: Particle method, MPS, hyperbolic-type weighting function, neural network, Laitone's approximate solutions, dam-breaking flow.

1 Introduction

The numerical fluid flow simulations have been successfully performed by many researchers with the use of finite difference method and finite element method based on grid/mesh-based frameworks [Stein, Borst and Hughes (2004)]. Numerical difficulties have been experienced in the solution of the Navier-Stokes equations at higher Reynolds numbers. In particular, it is well known that the centered finite difference and standard Galerkin finite element formulations lead to spurious oscillatory solutions for flow problem at high Reynolds number regimes. To overcome such spurious oscillations, various upwind/upstream-based schemes (in other words, Petrov-Galerkin method) have been consistently presented in both frameworks. On the other hand, in the framework of particle-based methodology, the appropriate choice of the weighting function (or kernel function) is indispensable in order to affect the behavior of the numerical solutions.

[1] College of Industrial Technology, Nihon University, Narashino, Chiba 275-8575, Japan.

There have been proposed various weighting functions (or kernel functions) in the gridless-based/meshless-based methods, such as SPH (Smoothed Particle Hydrodynamics) method [Lucy (1977); Gingold and Monaghan (1977)], MPS method [Koshizuka and Oka (1996)], MLPG (Meshless Local Petrov-Galerkin) method [Atluri and Zhu (1998); Lin and Atluri (2001); Avila and Atluri (2009); Avila, Han and Atluri (2011)], and LMFE (Lagrangian Meshless Finite Element) method [Idelsohn, Storti and Oñate (2001); Idelsohn, Oñate and Pin (2003); Idelsohn, Oñate and Pin (2004)], to simulate effectively complicated fluid flow problems. Some reviews of meshfree/particle methods and their applications have been presented excellently by Li and Liu [Li and Liu (2002)].

The SPH methods for solving compressible fluid flows with gravity have been firstly developed in the field of astrophysics, and applied successfully to a wide variety of complicated physical problems [Liu and Liu (2003)]. In the SPH-based framework, Lucy [Lucy (1977)] has used the bell-shaped function which satisfied some properties for the smoothing function to simulate the evolution of rotating protostar. The Gaussian kernel function without a compact support has been significantly proposed by Monaghan et al. [Gingold and Monaghan (1977); Monaghan (1988); Monaghan (1992)] to solve numerically the astrophysical complicated problems. Grenier et al. [Grenier, Antuono, Colagrossi, Touzé and Alessandrini (2009)] have presented a Gaussian kernel with a compact support to simulate the multi-fluid flows including free surface. Monaghan and Lattanzio [Monaghan and Lattanzio (1985)] have also presented the smoothing kernel based on the cubic spline functions, and higher-order spline functions have been widely adopted by many researchers [Morris, Fox and Zhu (1997); Cummins and Rudman (1999); Colagrossi and Landrini (2003); Tartakovsky, Meakin, Scheibe and West (2007); Koukouvinis, Anagnostopoulos and Papantonis (2013)]. The MPS method known as an incompressible fluid flow solver has been widely applied to the problem of breaking wave with large deformation, the fluid-structure interaction problem, and so forth. However, the standard MPS approach leads to the above-mentioned unphysical numerical oscillation of pressure fields which are described by the discretized Poisson equation. In the MPS-based framework, Koshizuka et al. [Koshizuka, Tamako and Oka (1995)] have firstly proposed a set of second-order polynomials as the kernel function to simulate numerically the collapse of a water column, namely the dam-breaking flow problem. Then, for the formulation of a standard MPS method, Koshizuka and Oka [Koshizuka and Oka (1996)] have proposed a kernel function with singularity, namely the function of inverse proportion with respect to the distance between two particles. The standard kernel function with singularity has been mainly used by some researchers [Liu, Koshizuka and Oka (2005); Khayyer and Gotoh (2009); Tanaka and Masunaga (2010); Khayyer and Gotoh (2012)]. We have proposed the MPS formulation using logarithmic-type weighting function to improve slightly the singularity of the kernel function [Kakuda, Obara, Toyotani, Meguro and Furuichi (2012); Kakuda, Nagashima, Hayashi, Obara, Toyotani, Katsurada, Higuchi and Matsuda (2012)]. Recently, a set of second-/third-order polynomial kernels without the singularity has been studied in the MPS-framework [Shakibaeinia and Jin (2010); Kondo and Koshizuka (2011); Lee, Park, Kim and Hwang (2011); Shakibaeinia and Jin (2012)] as with the application of the above-mentioned SPH-strategy. Atluri and Zhu [Atluri and Zhu (1998)] have developed the MLPG approach based on the local symmetric weak form and the moving least squares for solving accurately potential problems, and the approach was extended to deal with the problems for incompressible Navier-Stokes equations [Lin and Atluri (2001)] in fluid dynamics. Both Gaussian and spline weighting functions with the compact support have been effectively employed in the MLPG methodology. Avila and Atluri [Avila and Atluri (2009)] have presented efficiently various numerical solutions of the non-steady, two-dimensional Navier-Stokes equations by using the MLPG method coupled with a fully implicit pressure-correction approach. They have also proposed a novel MLPG-mixed finite volume method for solving the steady-state Stokes flow involving complex phenomena between eccentric rotating cylinders [Avila, Han and Atluri (2011)]. Valuable overviews of the MLPG method involving applications to fluid flows have been presented in detail by Sladek et al. [Sladek, Stanak, Han, Sladek and Atluri (2013)]. A group of Idelsohn et al. [Idelsohn, Storti and Oñate (2001); Idelsohn, Oñate and Pin (2003); Idelsohn, Oñate and Pin (2004)] has developed expertly the LMFE method for solving incompressible fluid flows with free surfaces and applied to complex problems including the dam-breaking flow and fluid-structure interactions. They have used the polynomial interpolation functions based on the Galerkin finite element formulation.

The purpose of this paper is to propose a hyperbolic-type weighting function to formulate the particle method based on the MPS. The hyperbolic-type weighting function with the compact support is constructed by differentiating the characteristic function (i.e., sigmoid function) based on neural network framework [Rumelhart, Hinton and Williams (1986); Funahashi (1989)]. And also, the weighting function has the form similar to Laitone's approximate solutions for a solitary wave [Laitone (1960)], which are often used for comparative studies [Ramaswamy (1990); Hansbo (1992); Radovitzky and Ortiz (1998); Duarte, Gormaz and Natesan (2004); Nithiarasu (2005)]. The weighting function which has the property of Dirac delta function is concomitantly applied to the smoothing kernel function in the SPH-framework. The workability and validity of the present MPS approach are demonstrated through the dam-breaking flow problem [Martin and Moyce (1952);

Hirt and Nichols (1981); Ramaswamy and Kawahara (1987)], and compared with experimental data and other numerical ones.

Throughout this paper, the summation convention on repeated indices is employed. A comma following a variable is used to denote partial differentiation with respect to the spatial variable.

2 Statement of the problem and the standard MPS formulation

Let Ω be a bounded domain in 2D/3D Euclidean space with a piecewise smooth boundary Γ. The unit outward normal vector to Γ is denoted by $\boldsymbol{n}$. And also, $\Im$ denotes a closed time interval.

The motion of an incompressible viscous fluid flow is governed by the following Navier-Stokes equations :

$$\frac{Du_i}{Dt} = -\frac{1}{\rho}p_{,i} + \nu u_{i,jj} + f_i \qquad in\, \Im \times \Omega \tag{1}$$

$$\frac{D\rho}{Dt} = 0 \qquad in\, \Im \times \Omega \tag{2}$$

where u_i is the velocity vector component, ρ is the density, p is the pressure, f_i is the external force, e.g., gravity, ν is the kinematic viscosity, and D/Dt denotes the Lagrangian differentiation. In addition to Eq. 1 and Eq. 2, we prescribe the initial condition $u_i(\boldsymbol{x},0) = u_i^0$, where u_i^0 denotes the given initial velocity, and the Dirichlet and Neumann boundary conditions.

In this stage, let us briefly describe the standard MPS as one of the meshfree particle methods [Koshizuka and Oka (1996)]. The particle interaction models of the MPS as illustrated in Fig. 1(a) are prepared with respect to differential operators, namely gradient, divergence and Laplacian. The incompressible viscous fluid flow is calculated by a semi-implicit algorithm, such as SMAC (Simplified MAC) scheme [Amsden and Harlow (1970)].

The particle number density n at particle i with the neighboring particles j is defined as

$$< n >_i = \sum_{j \neq i} w(|\boldsymbol{r}_j - \boldsymbol{r}_i|) \tag{3}$$

in which w denotes the following kernel function (or weighting function) with the compact support as shown in Fig. 1(b)

$$w(r) = \begin{cases} \dfrac{r_e}{r} - 1 & (0 < r < r_e) \\ 0 & (r_e \leq r) \end{cases} \tag{4}$$

where r_e is *ad hoc* influence radius as shown in Fig. 1(a).

The model of the gradient vectors at particle i between particles i and j is weighted with the kernel function and averaged as follows:

$$< \nabla\phi >_i = \frac{d}{n^0}\sum_{j\neq i}\left[\frac{\phi_j-\phi_i}{|\boldsymbol{r}_j-\boldsymbol{r}_i|^2}(\boldsymbol{r}_j-\boldsymbol{r}_i)w(|\boldsymbol{r}_j-\boldsymbol{r}_i|)\right] \quad (5)$$

where d is the number of spatial dimensions, ϕ_i and ϕ_j denote the scalar quantities at coordinates $\boldsymbol{r}_i$ and $\boldsymbol{r}_j$, respectively, and n^0 is the constant value of the particle number density. The Laplacian model at particle i is also given by

$$< \nabla^2\phi >_i = \frac{2d}{n^0\lambda}\sum_{j\neq i}(\phi_j-\phi_i)w(|\boldsymbol{r}_j-\boldsymbol{r}_i|) \quad (6)$$

where λ is an *ad hoc* coefficient.

The Poisson equation for solving implicitly the pressure field at particle i is given as follows:

$$< \nabla^2 p >_i = -\frac{\rho}{\Delta t^2}\frac{< n^* >_i - n^0}{n^0} \quad (7)$$

where $< n^* >_i$ denotes the particle number at particle i.

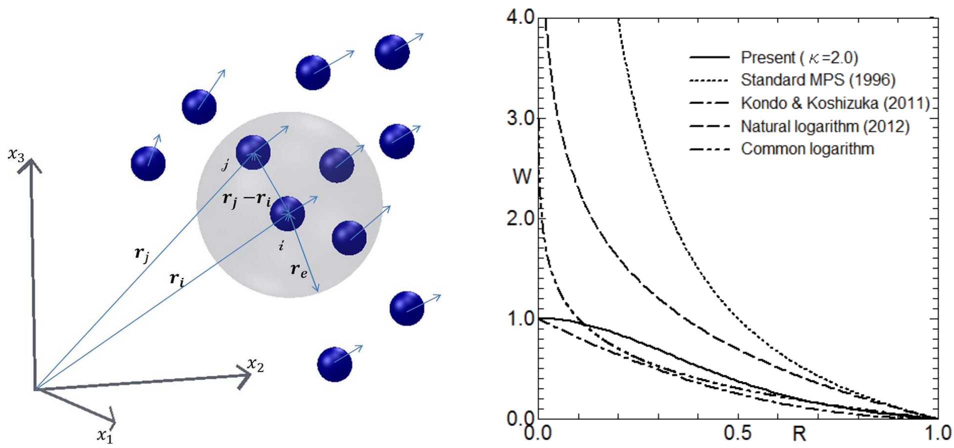

(a) Particle interaction models (3D) (b) Profiles of weighting functions

Figure 1: Particle interaction models and weighting functions

3 Construction of the hyperbolic-type weighting function

For the MPS formulation, the appropriate choice of a weighting function is a key factor in the particle-based simulations. If the distance r between the coordinates $\boldsymbol{r}_i$ and $\boldsymbol{r}_j$ is very close, then there is a possibility that the computation fails suddenly with unphysical numerical oscillations. Therefore, in order to stabilize such spurious oscillations generated by the above-mentioned standard MPS strategy, we have used the following logarithmic-type weighting function as shown in Fig. 1(b), and also considered the reduction of *ad hoc* influence radius, r_e, for solving the pressure fields [Kakuda, Obara, Toyotani, Meguro and Furuichi (2012)].

$$w(r) = \begin{cases} ln(\frac{r_e}{r}) & (0 < r < r_e) \\ 0 & (r_e \le r) \end{cases} \tag{8}$$

The common logarithmic-type weighting function is also similar to the profile of the weighting function presented by Kondo and Koshizuka to stabilize the pressure calculations [Kondo and Koshizuka (2011)](see Fig. 1(b)).

However, we propose newly the following hyperbolic-type weighting function instead of the logarithmic-type weighting function which has a singularity.

$$w(r) = \begin{cases} \theta \dfrac{sech^2(\frac{\kappa r}{r_e}) - sech^2(\kappa)}{1 - sech^2(\kappa)} & (0 \le r < r_e) \\ 0 & (r_e \le r) \end{cases} \tag{9}$$

where θ and κ denote *ad hoc* parameters. In Fig. 1(b) and Fig. 2, we show also the profiles of Eq. 9 for the parameters κ and $\theta = 1$, in which $R = r/r_e$.

The hyperbolic-type weighting function with the compact support is constructed by differentiating the characteristic function based on neural network framework. In the following, we shall describe the derivation of the function.

In the field of neural networks, the input-output relationship known as the back-propagation is represented by inputs U_j, output V_j and the characteristic function h as follows:

$$V_j = h(U_j) \tag{10}$$

$$U_j = \sum_{i=1}^{n} S_{ij} w_{ij} + I_j - T_j \tag{11}$$

where S_{ij} are j-th input values as shown in Fig. 3, w_{ij} are the connection weights, I_j is the bias value and T_j denotes threshold. The sigmoid function (see Fig. 4(a)) has

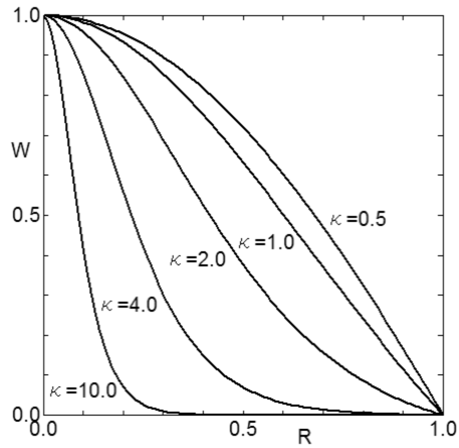

Figure 2: Profiles of Eq. 9 for the parameters κ and $\theta = 1$

been mainly used as the continuous characteristic function h [Rumelhart, Hinton and Williams (1986); Funahashi (1989)].

$$h(v) = \frac{1}{2}(1 + tanh(\frac{v}{2k})) \tag{12}$$

By differentiating with respect to the variable v of Eq. 12, we obtain the form as follows (see Fig. 4(b)):

$$h'(v) = \frac{1}{4k} sech^2(\frac{v}{2k}) \tag{13}$$

In order to relate the particle-based formulation and Eq. 13, we put as follows:

$$v = r \quad , \quad k = \frac{r_e}{2\kappa} \tag{14}$$

and also assume the following weighting function to satisfy the compact support property (if $r/r_e = 1$, then $w = 0$, i.e, $w(r)_{/r=r_e} = 0$.) [Liu and Liu (2003)]:

$$w(r) = a_0 + \frac{a_1\kappa}{2r_e} sech^2(\frac{\kappa r}{r_e}) \tag{15}$$

Consequently, we obtain the form of Eq. 9 by solving the coefficients a_0 and a_1 from the conditions of the compact support and $w(r)_{/r=0} = \theta$.

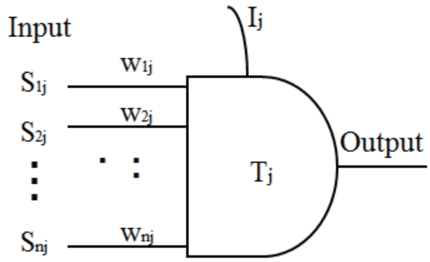

Figure 3: Neuron model

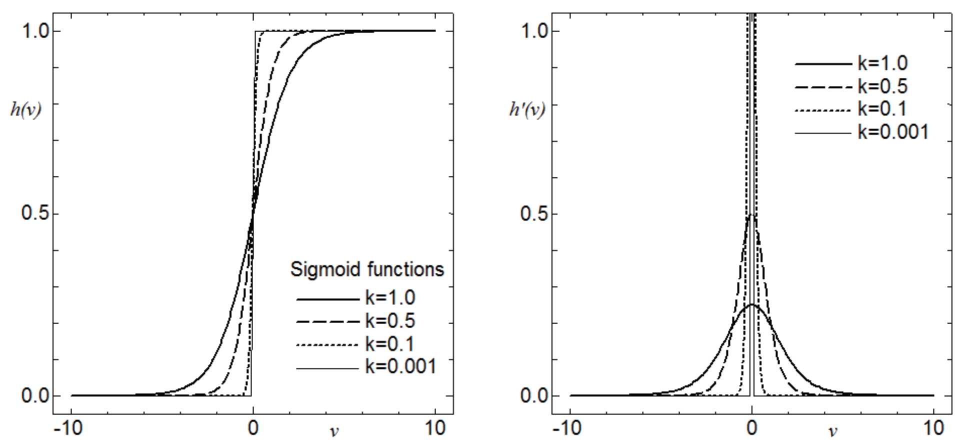

(a) Sigmoid functions (b) Profiles of Eq. 13

Figure 4: Sigmoid functions and profiles of Eq. 13

4 Application to the kernel function in SPH

The smoothing function of Eq. 13 has the property of Dirac delta function as the length r_e or k approaches to zero shown in Fig. 4(b). Therefore, the above-mentioned hyperbolic function can be also applied to the construction of the kernel function with other properties, namely the normalization/unity and the compact support properties, and so forth [Liu and Liu (2003)].

In one-dimensional (1D) space, the form of Eq. 15 can be written by using the normalization/unity condition as follows:

$$2\int_0^{2r_e}\{a_0+\frac{a_1\kappa}{2r_e}sech^2(\frac{\kappa r}{r_e})\}dr=1 \tag{16}$$

And also, for the smoothing function W to have the compact support condition $W(R,r_e)_{/R=2}=0$, we have as follows:

$$a_0+\frac{a_1\kappa}{2r_e}sech^2(2\kappa)=0 \tag{17}$$

Solving Eq. 16 and Eq. 17, the coefficients a_0 and a_1 are obtained as

$$a_0=-\frac{a_1\kappa}{2r_e}sech^2(2\kappa) \quad , \quad a_1=\frac{1}{tanh(2\kappa)-2\kappa\, sech^2(2\kappa)} \tag{18}$$

As a result, we find the smoothing kernel function as follows:

$$W(R,r_e)=\frac{a_1\kappa}{2r_e}\{sech^2(\kappa R)-sech^2(2\kappa)\} \qquad (0\leq R<2) \tag{19}$$

Similarity, we can derive the coefficient a_1 in the kernel function of Eq. 19, respectively, for 2D space (see Fig. 5)

$$a_1=\frac{1}{\pi r_e[\frac{1}{\kappa}\{2\kappa\, tanh(2\kappa)-ln(cosh(2\kappa))\}-2\kappa\, sech^2(2\kappa)]} \tag{20}$$

and for 3D space

$$a_1=\frac{1}{2\pi r_e^2[\frac{1}{\kappa^2}\mathscr{L}-\frac{8\kappa}{3}sech^2(2\kappa)]} \tag{21}$$

in which

$$\mathscr{L}=4\kappa^2\{tanh(2\kappa)-1\}-4\kappa\, ln(e^{-4\kappa}+1)+Li_2(-e^{-4\kappa})+\frac{\pi^2}{12} \tag{22}$$

where $Li_2(x)$ denotes the polylogarithm function [Olver, Lozier, Boisvert and Clark (2010)].

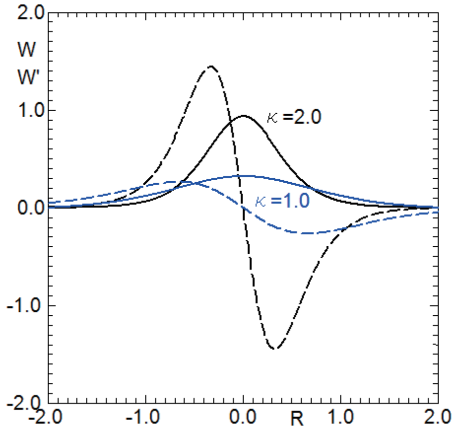

Figure 5: Profiles of the kernel function and its derivative for 2D space

5 Numerical examples

In this section we present numerical results obtained from applications of the above-mentioned MPS method to incompressible viscous fluid flow problems, namely dam-breaking flow problem involving free surface and gravity. Some experimental data have been presented in the dam-breaking flow or the collapse of a liquid column [Martin and Moyce (1952); Koshizuka, Tamako and Oka (1995); Cruchaga, Celentano and Tezduyar (2007)]. The dam-breaking flow problem has been extensively used to verify the applicability and validity of the numerical methods. The initial velocities are assumed to be zero everywhere in the interior domain. In 2D/3D simulations, we set the CFL condition $u_{max}\Delta t/l_{min} \leq C$, where C is the Courant number. The kernel size for the particle number density and the gradient/Laplacian models is $r_e = 4.0l_0$, in which l_0 is the distance between two neighboring particles in the initial state, and we use different parameters, κ, for velocity and pressure calculations, respectively. Recently, the Poisson equation for solving accurately the pressure field at particle i is also presented by Kondo and Koshizuka [Kondo and Koshizuka (2011)]. In this case, we set $l_0 = 0.008m$ and also $(\beta,\gamma) = (0.5, 0.05)$.

5.1 2D dam-breaking flow simulation

Let us consider 2D simulation using the improved approach for flow in the dam-breaking problem. Fig. 6 shows the geometry and the initial state of particles for the dam-breaking flow problem. In this two-dimensional simulation, we set $1,632$

particles in the initial configuration with the kinematic viscosity of $1.0 \times 10^{-6} m^2/s$, and also $\kappa = 2$ *or* 3 and $\kappa = 4$ for velocity and pressure calculations, respectively. The standard MPS method leads to irregular pressure distributions from early times (see, Fig. 7(a)), while the present behaviors as shown in Fig. 7(c) and (d) are improved as well as the results of Fig. 7(b) [Kakuda, Obara, Toyotani, Meguro and Furuichi (2012)]. The present behaviors for $\kappa = 2$ in Fig. 7(c) are similar to the results obtained by using MPS method with logarithmic-type weighting function. The particle and pressure behaviors for $\kappa = 2$ at different time are also shown in Fig. 8. Fig. 9 shows the comparisons with the time histories of the pressure at particles A and B as shown in Fig. 6(b). We can see from Fig. 9 that the pressure behaviors at particles A and B are smoother and higher than the standard MPS calculations. Fig. 10 shows the time evolutions of the leading-edge of the water using present approach and standard MPS method through comparison with experimental data [Martin and Moyce (1952)], in which $T = t\sqrt{2g/L}$. The agreement between the present results and the experimental data appears satisfactory.

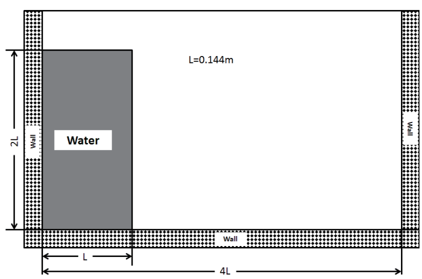

(a) Geometrical configuration

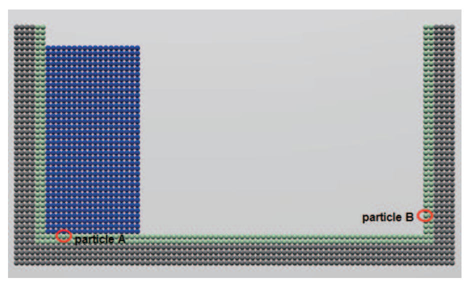

(b) Initial state of particles

(c) Pressure color-bar

Figure 6: Dam-breaking flow configuration for 2D simulation

5.2 3D dam-breaking flow simulation

Let us next consider 3D simulation using the improved approach for flow in the dam-breaking problem. Fig. 11 shows the geometry and the initial state of particles 75,744 for the dam-breaking flow problem with the kinematic viscosity of $1.0 \times 10^{-6} m^2/s$. In this approach, we set also $\kappa = 2$ *or* 3 and $\kappa = 4$ for velocity and pressure calculations, respectively. The particle and pressure behaviors for $\kappa = 2$ at different time are shown in Fig. 12, and more smoother results are obtained certainly by means of the present approach. In Fig. 13, we give the comparisons with

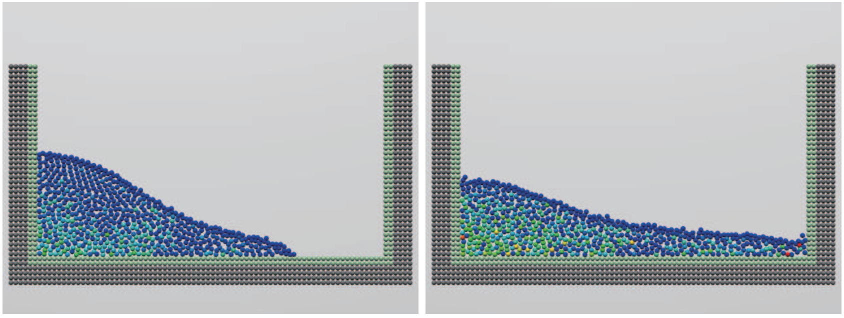

(a) Standard MPS method

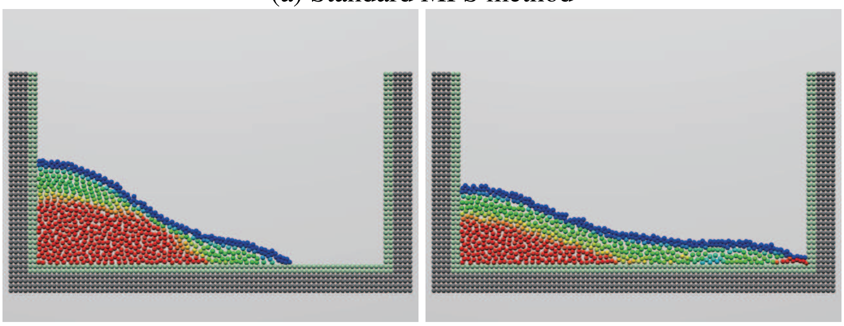

(b) MPS using logarithmic-type weighting function [Kakuda, et. al. (2012)]

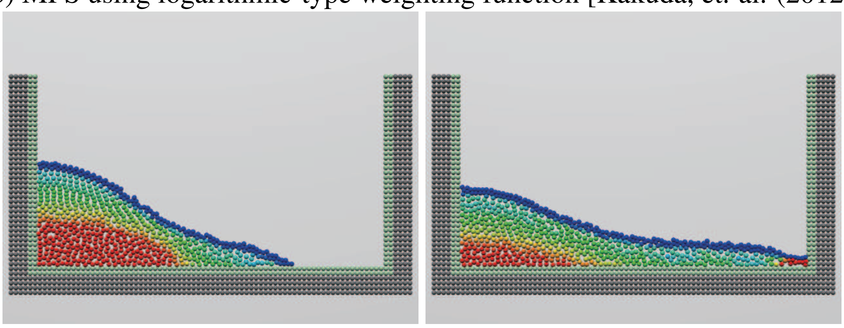

(c) MPS using hyperbolic-type weighting function with $\kappa = 2/\kappa = 4$

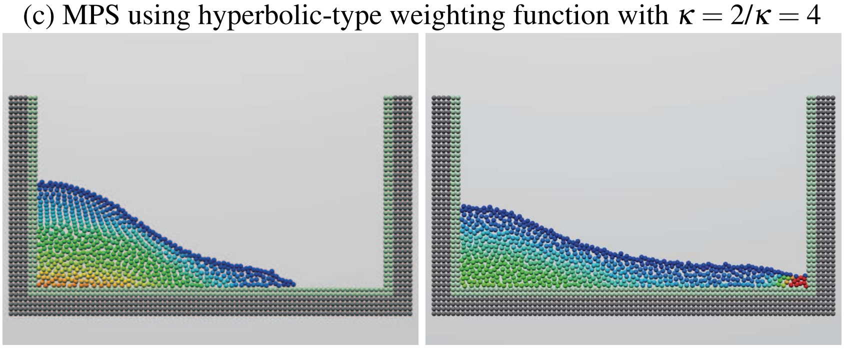

(d) MPS using hyperbolic-type weighting function with $\kappa = 3/\kappa = 4$

Figure 7: Particle and pressure behaviors at time $t \approx 0.19s$ (left) and $0.26s$ (right)

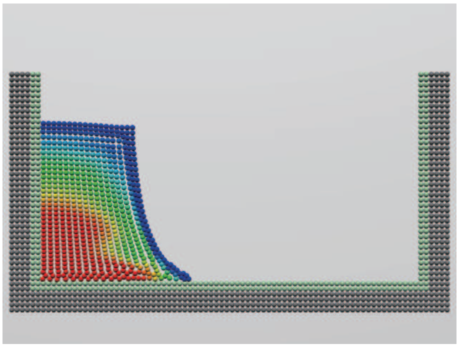

(a) $t \approx 0.09s$

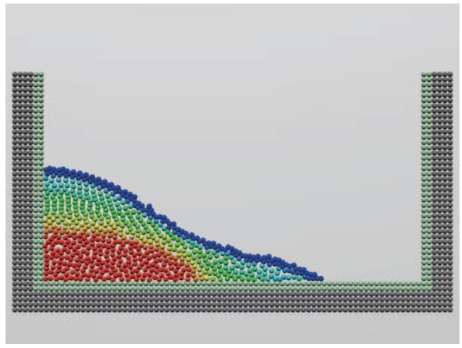

(b) $t \approx 0.19s$

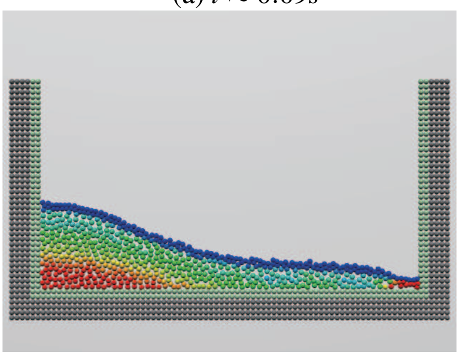

(c) $t \approx 0.26s$

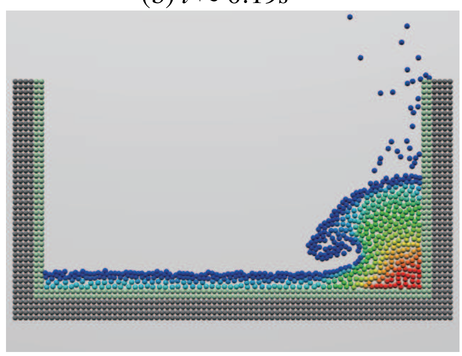

(d) $t \approx 0.69s$

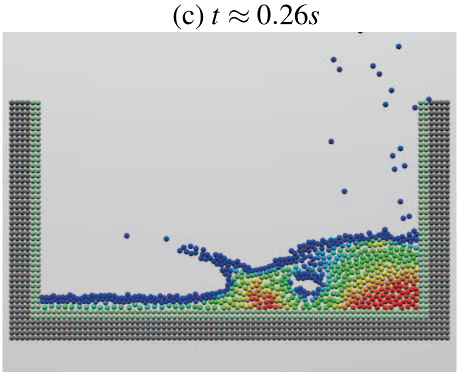

(e) $t \approx 0.79s$

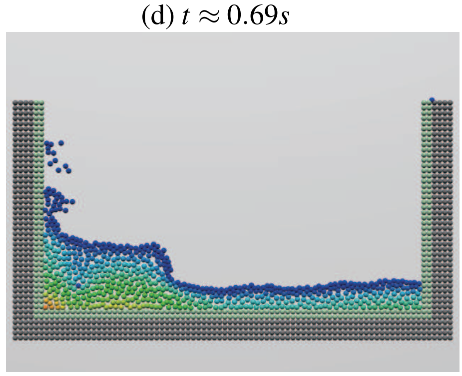

(f) $t \approx 1.19s$

Figure 8: Particle and pressure behaviors for $\kappa = 2/\kappa = 4$ at different time (2D)

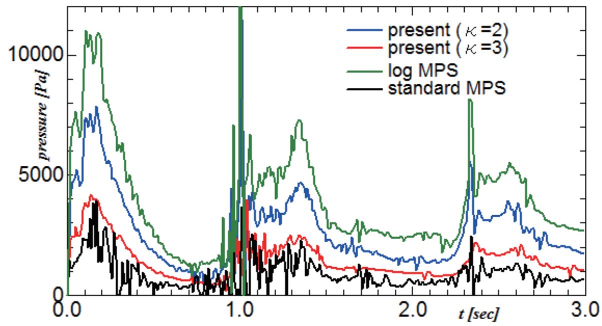

(a) Time histories of the pressure at particle *A*

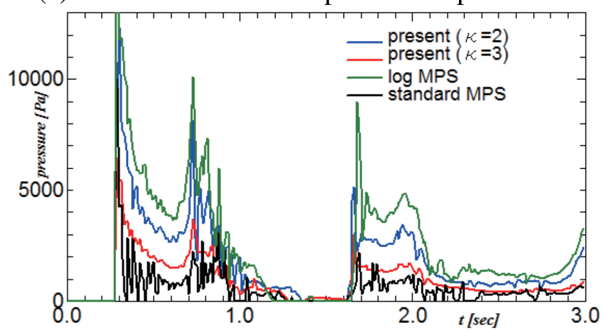

(b) Time histories of the pressure at particle *B*

Figure 9: Comparisons of time histories of the pressure at particles *A* and *B*

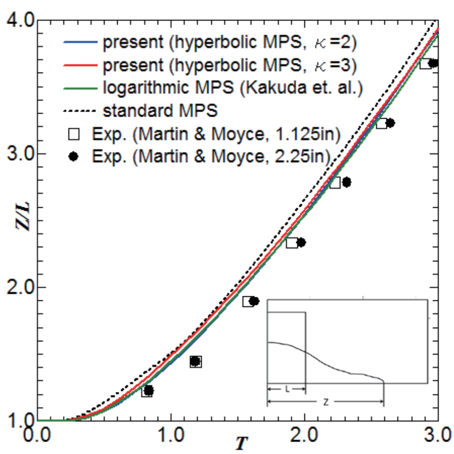

Figure 10: Comparisons with experimental and other data (2D)

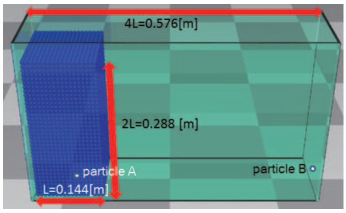

(a) Geometrical configuration

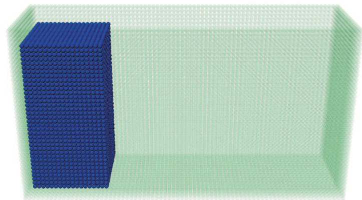

(b) Initial state of particles

(c) Pressure color-bar

Figure 11: Dam-breaking flow configuration for 3D simulation

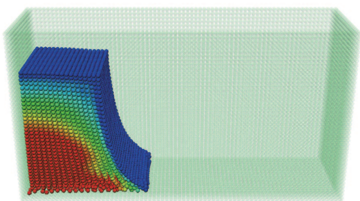

(a) $t \approx 0.09s$

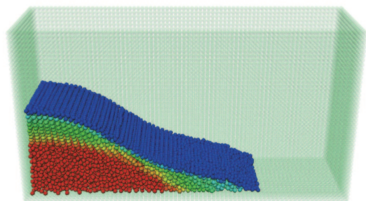

(b) $t \approx 0.19s$

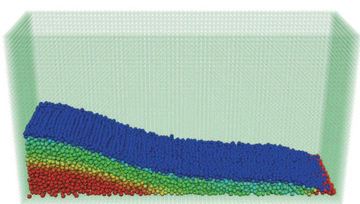

(c) $t \approx 0.26s$

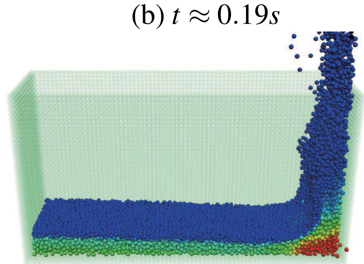

(d) $t \approx 0.49s$

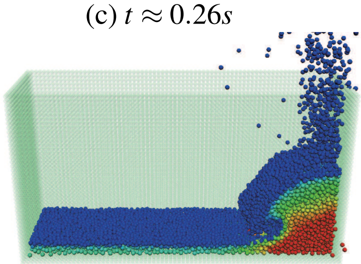

(e) $t \approx 0.69s$

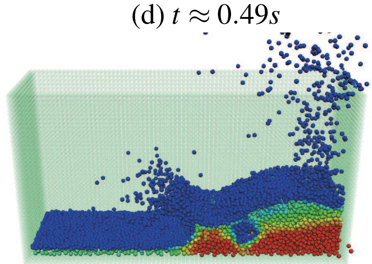

(f) $t \approx 0.79s$

Figure 12: Particle and pressure behaviors for $\kappa = 2/\kappa = 4$ at different time (3D)

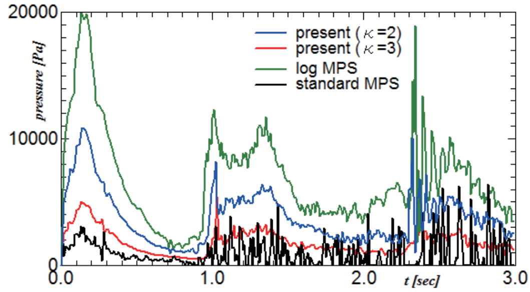

(a) Time histories of the pressure at particle *A*

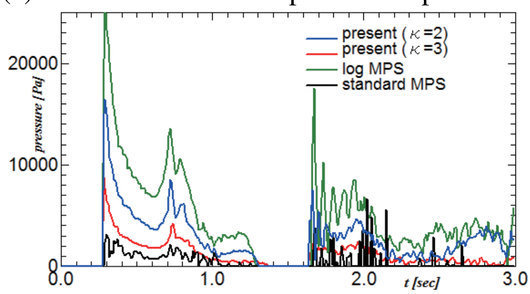

(b) Time histories of the pressure at particle *B*

Figure 13: Comparisons of time histories of the pressure at particles *A* and *B*

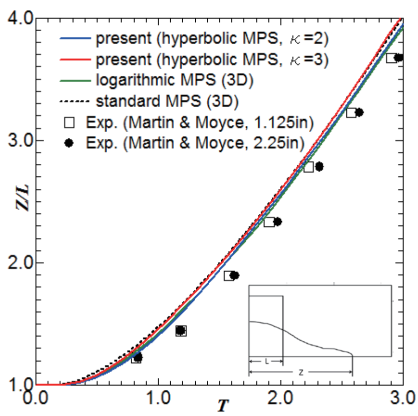

(a) Results of 3D simulations

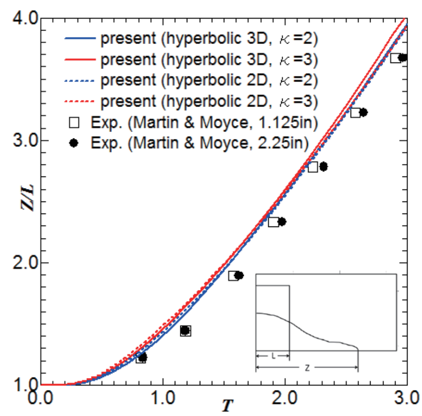

(b) Comparisons with 2D and 3D results

Figure 14: Comparisons with experimental and other data

the time histories of the pressure at particles *A* and *B* as shown in Fig. 11(a). The present results of 3D simulation are qualitatively similar to the behaviors obtained from 2D approach (see, Fig. 9). Fig. 14 shows the time evolutions of the leading-edge of the water using present approach and standard MPS method through comparison with the experimental data, and also the comparisons with results of 2D and 3D simulations. The correlation between the present results for $\kappa = 2$ and the experimental data appears satisfactory (see, Fig. 14(a)). The present profiles of both 2D/3D results for $\kappa = 2$ as shown in Fig. 14(b) agree generally well with the experimental data.

6 Conclusions

We have presented the MPS approach using hyperbolic-type weighting function for solving numerically 2D/3D incompressible viscous fluid flow of the broken dam problem with free surfaces. The standard MPS scheme has been widely utilized as a particle strategy for free surface flow, the problem of moving boundary, and multi-physics/multi-scale ones. To overcome spurious oscillations in the standard MPS method, we have proposed to utilize the hyperbolic-type weighting function and also use *ad hoc* different parameters, κ, for velocity and pressure calculations, respectively. The hyperbolic-type weighting function which had the form similar to Laitone's approximate solutions has been constructed by differentiating the characteristic function (i.e., sigmoid function) based on neural network framework. The weighting function with the property of Dirac delta function has been consistently applied to the smoothing kernel function in the SPH-framework.

As the numerical example, the well-known 2D/3D dam-breaking flow simulations were carried out and compared with experimental data and other data. The particle and pressure behaviors at different time have been significantly presented by using our approach through comparison with the experimental time-evolutions of the leading-edge of the water. The qualitative agreement between our 2D/3D simulations and experimental data appeared very satisfactory.

Acknowledgement: This work was supported by Grant-in-Aid for Scientific Research (C) (KAKENHI:No.23560075) in the MEXT.

References

Amsden, A. A.; Harlow, F. H. (1970): A simplified MAC technique for incompressible fluid flow calculations. *J. Comput. Phys.*, vol.6, pp.322–325.

Atluri, S. N.; Zhu, T. (1998): A new meshless local Petrov-Galerkin (MLPG) approach in computational mechanics. *Comput. Mech.*, vol.22, pp.117–127.

Avila, R.; Atluri, S. N. (2009): Numerical solution of non-steady flows, around surfaces in spatially and temporally arbitrary motions, by using the MLPG method. *CMES: Computer Modeling in Engineering & Sciences*, vol.54, no.1, pp.15–64.

Avila, R.; Han, Z.; Atluri, S. N. (2011): A novel MLPG-finite-volume mixed method for analyzing Stokesian flows & study of a new vortex mixing flow. *CMES: Computer Modeling in Engineering & Sciences*, vol.71, no.4, pp.363–395.

Colagrossi, A.; Landrini, M. (2003): Numerical simulation of interfacial flows by smoothed particle hydrodynamics. *J. Comput. Phys.*, vol.191, pp.448–475.

Cruchaga, M. A.; Celentano, D. J.; Tezduyar, T. E. (2007): Collapse of a liquid colummn: numerical simulation and experimental validation. *Comput. Mech.*, vol.39, pp.453–476.

Cummins, S. J.; Rudman, M. (1999): An SPH projection method. *J. Comput. Phys.*, vol.152, pp.584–607.

Duarte, F.; Gormaz, R.; Natesan, S. (2004): Arbitrary Lagrangian-Eulerian method for Navier-Stokes equations with moving boundaries. *Comput. Methods Appl. Mech. Engrg.*, vol.193, pp.4819–4836.

Funahashi, K. (1989): On the approximate realization of contnuous mappings by neural networks. *Neural Networks*, vol.2, pp.183–192.

Gingold, R. A.; Monaghan, J. J. (1977): Smoothed particle hydrodynamics: theory and application to non-spherical stars. *Mon. Not. R. astr. Soc.*, vol.181, pp.375–389.

Grenier, N.; Antuono, M.; Colagrossi, A.; Touzé, D. L.; Alessandrini, B. (2009): An Hamiltonian interface SPH formulation for multi-fluid and free surface flows. *J. Comput. Phys.*, vol.228, pp.8380–8393.

Hansbo, P. (1992): The characteristic streamline diffusion method for the time-dependent incompressible Navier-Stokes equations. *Comput. Methods Appl. Mech. Engrg.*, vol.99, pp.171–186.

Hirt, C. W.; Nichols, B. D. (1981): Volume of fluid (VOF) method for the dynamics of free boundaries. *J. Comput. Phys.*, vol.39, pp.201–225.

Idelsohn, S. R.; Storti, M. A.; Oñate, E. (2001): Lagrangian formulations to solve free surface incompressible inviscid fluid flows. *Comput. Methods Appl. Mech. Engrg.*, vol.191, pp.583–593.

Idelsohn, S. R.; Oñate, E.; Pin, F. Del (2003): A Lagrangian meshless finite element method applied to fluid-structure interaction problems. *Comput. Struct.*, vol.81, pp.655–671.

Idelsohn, S. R.; Oñate, E.; Pin, F. Del (2004): The particle finite element method: a powerful tool to solve incompressible flows with free-surfaces and breaking waves. *Int. J. Numer. Meth. Engng.*, vol.61, pp.964–989.

Kakuda, K.; Obara, S.; Toyotani, J.; Meguro, M.; Furuichi, M. (2012): Fluid flow simulation using particle method and its physics-based computer graphics. *CMES: Computer Modeling in Engineering & Sciences*, vol.83, no.1, pp.57–72.

Kakuda, K.; Nagashima, T.; Hayashi, Y.; Obara, S.; Toyotani, J.; Katsurada, N.; Higuchi, S.; Matsuda, S. (2012): Particle-based fluid flow simulations on GPGPU using CUDA. *CMES: Computer Modeling in Engineering & Sciences*, vol.88, no.1, pp.17–28.

Khayyer, A.; Gotoh, H. (2009): Modified moving particle semi-implicit methods for the prediction of 2d wave impact pressure. *Coastal Engineering*, vol.56, pp.419–440.

Khayyer, A.; Gotoh, H. (2012): A 3D higher order Laplacian model for enhancement and stabilization of pressure calculation in 3D MPS-based simulations. *Applied Ocean Research*, vol.37, pp.120–126.

Kondo, M.; Koshizuka, S. (2011): Improvement of stability in moving particle semi-implicit method. *Int. J. Numer. Meth. Fluids*, vol.65, pp.638–654.

Koshizuka, S.; Oka, Y. (1996): Moving-particle semi-implicit method for fragmentation of incompressible fluid. *Nucl. Sci. Eng.*, vol.123, pp.421–434.

Koshizuka, S.; Tamako, H.; Oka, Y. (1995): A particle method for incompressible viscous flow with fluid fragmentation. *Comput. Fluid Dynamics J.*, vol.4, no.1, pp.29–46.

Koukouvinis, P. K.; Anagnostopoulos, J. S.; Papantonis, D. E. (2013): An improved MUSCL treatment for the SPH-ALE method: comparison with the standard SPH method for the jet impingement case. *Int. J. Numer. Meth. Fluids*, vol.71, pp.1152–1177.

Lee, B. H.; Park, J. C.; Kim, M. H.; Hwang, S. C. (2011): Step-by-step improvement of MPS method in simulating violent free-surface motions and impact-loads. *Comput. Methods Appl. Mech. Engrg.*, vol.200, pp.1113–1125.

Laitone, E. V. (1960): The second approximation to cnoidal and solitary waves. *J. Fluid Mech.*, vol.9, pp.430–444.

Li, S.; Liu, W. K. (2002): Meshfree and particle methods and their applications. *Appl. Mech. Rev.*, vol.55, no.1, pp.1–34.

Lin, H.; Atluri, S. N. (2001): The meshless local Petrov-Galerkin (MLPG) method for solving incompressible Navier-Stokes equations. *CMES: Computer Modeling in Engineering & Sciences*, vol.2, no.2, pp.117–142.

Liu, J.; Koshizuka, S.; Oka, Y. (2005): A hybrid particle-mesh method for viscous, incompressible, multiphase flows. *J. Comput. Phys.*, vol.202, pp.65–93.

Liu, G. R.; Liu, M. B. (2003): Smoothed particle hydrodynamics: a meshfree particle method. *World Scientific*, New Jersey, ISBN-13 978-981-238-456-0.

Lucy, L. B. (1977): A numerical approach to the testing of the fission hypothesis. *The Astronomical J.*, vol.82, no.12, pp.1013–1024.

Martin, J. C.; Moyce, W. J. (1952): An experimental study of the collapse of liquid columns on a rigid horizontal plane. *Philos. Trans. R. Soc. London Ser. A*, vol.244, pp.312–334.

Monaghan, J. J. (1988): An introduction to SPH. *Comput. Phys. Commun.*, vol.48, pp.89–96.

Monaghan, J. J. (1992): Smoothed particle hydrodynamics. *Annu. Rev. Astron. Astrophys.*, vol.30, pp.543–574.

Monaghan, J. J.; Lattanzio, J. C. (1985): A refined particle method for astrophysical problems. *Astronomy and Astrophysics*, vol.149, pp.135–143.

Morris, J. P.; Fox, P. J.; Zhu, Y. (1997): Modeling low Reynolds number incompressible flows using SPH. *J. Comput. Phys.*, vol.136, pp.214–226.

Nithiarasu, P. (2005): An arbitrary Lagrangian Eulerian (ALE) formulation for free surface flows using the characteristic-based split (CBS) scheme. *Int. J. Numer. Meth. Fluids*, vol.48, pp.1415–1428.

Olver, F. W. J.; Lozier, D. W.; Boisvert, R. F.; Clark, C. W. (2010): NIST handbook of mathematical functions. *Cambridge University Press*, ISBN 978-0-521-14063-8.

Radovitzky, R.; Ortiz, M. (1998): Lagrangian finite element analysis of Newtonian fluid flows. *Int. J. Numer. Meth. Engng.*, vol.43, pp.607–619.

Ramaswamy, B. (1990): Numerical simulation of unsteady viscous free surface flow. *J. Comput. Phys.*, vol.90, pp.396–430.

Ramaswamy, B.; Kawahara, M. (1987): Lagrangian finite element analysis applied to viscous free surface fluid flow. *Int. J. Numer. Meth. Fluids*, vol.7, pp.953–984.

Rumelhart, D. E.; Hinton, G. E.; Williams, R. J. (1986): Learning representations by back-propagating errors. *Nature*, vol.323, pp.533–536.

Shakibaeinia, A.; Jin, Y. C. (2010): A weakly compressible MPS method for modeling of open-boundary free-surface flow. *Int. J. Numer. Meth. Fluids*, vol.63, pp.1208–1232.

Shakibaeinia, A.; Jin, Y. C. (2012): MPS mesh-free particle method for multiphase flows. *Comput. Methods Appl. Mech. Engrg.*, vol.229-232, pp.13–26.

Sladek, J.; Stanak, P.; Han, Z.-D.; Sladek, V.; Atluri, S. N. (2013): Applications of the MLPG method in engineering & sciences: a review. *CMES: Computer Modeling in Engineering & Sciences*, vol.92, no.5, pp.423–475.

Stein, E; de Borst, R.; Hughes, T. J. R.. (2004): Encyclopedia of computational mechanics. *Vol.3 Fluids*, John Wiley & Sons, ISBN 0-470-84699-2.

Tanaka, M.; Masunaga, T. (2010): Stabilization and smoothing of pressure in MPS method by quasi-compressibility. *J. Comput. Phys.*, vol.229, pp.4279–4290.

Tartakovsky, A. M.; Meakin, P.; Scheibe, T. D.; West, R. M. E. (2007): Simulations of reactive transport and precipitation with smoothed particle hydrodynamics. *J. Comput. Phys.*, vol.222, pp.654–672.